Quantum computation algorithm for many-body studies

E. Ovrum and M. Hjorth-Jensen

Department of Physics and Center of Mathematics for Applications, University of Oslo, N-0316 Oslo, Norway
(Dated: January 5, 2014)

We show in detail how the Jordan-Wigner transformation can be used to simulate any fermionic many-body Hamiltonian on a quantum computer. We develop an algorithm based on appropriate qubit gates that takes a general fermionic Hamiltonian, written as products of a given number of creation and annihilation operators, as input. To demonstrate the applicability of the algorithm, we calculate eigenvalues and eigenvectors of two model Hamiltonians, the well-known Hubbard model and a generalized pairing Hamiltonian. Extensions to other systems are discussed.

I. INTRODUCTION

A theoretical understanding of the behavior of many-body systems is a great challenge and provides fundamental insights into quantum mechanical studies, as well as offering potential areas of applications. However, apart from some few analytically solvable problems, the typical absence of an exactly solvable contribution to the many-particle Hamiltonian means that we need reliable numerical many-body methods. These methods should allow for controlled approximations and provide a computational scheme which accounts for successive many-body corrections in a systematic way. Typical examples of popular many-body methods are coupled-cluster methods [1, 2, 3], various types of Monte Carlo methods [4, 5, 6], perturbative expansions [7, 8], Green's function methods [9, 10], the density-matrix renormalization group [11, 12], ab initio density functional theory [13, 14, 15] and large-scale diagonalization methods [16, 17, 18, 19].

However, all these methods have to face in some form or the other the problem of an exponential growth in dimensionality. For a system of P fermions which can be placed into N levels, the total number of basis states are given by $\begin{pmatrix} N \\ P \end{pmatrix}$. The dimensional curse means that most quantum mechanical calculations on classical computers have exponential complexity and therefore are very hard to solve for larger systems. On the other hand, a so-called quantum computer, a particularly dedicated computer, can improve greatly on the size of systems that can be simulated, as foreseen by Feynman [22, 23]. A quantum computer does not need an exponential amount of memory to represent a quantum state. The basic unit of information for a quantum computer is the so-called qubit or quantum bit. Any suitable two-level quantum system can be a qubit, but the standard model of quantum computation is a model where two-level quantum systems are located at different points in space, and are manipulated by a small universal set of operations. These operations are called gates in the same fashion as operations on bits in classical computers are called gates.

For the example of P spin 1/2 particles, a classical computer needs 2^P bits to represent all possible states, while a quantum computer needs only P qubits. The complexity in number of qubits is thus linear. Based

on these ideas, several groups have proposed various algorithms for simulating quantal many-body systems on quantum computers. Abrams and Lloyd, see for example Refs. [20, 21], introduced a quantum algorithm that uses the quantum fast Fourier transform to find eigenvalues and eigenvectors of a given Hamiltonian, illustrating how one could solve classically intractable problems with less than 100 qubits. Achieving a polynomial complexity in the number of operations needed to simulate a quantum system is not that straightforward however. To get efficient simulations in time one needs to transform the many-body Hamiltonian into a sum of operations on qubits, the building blocks of the quantum simulator and computer, so that the time evolution operator can be implemented in polynomial time. In Refs. [24, 25, 26] it was shown how the Jordan-Wigner transformation in principle does this for all Hamiltonians acting on fermionic many-body states. Based on this approach, recently two groups, see Refs. [27, 28], published results where they used Nuclear Magnetic Resonance (NMR) qubits to simulate the pairing Hamiltonian.

The aim of this work is to develop an algorithm than allows one to perform a quantum computer simulation (or simply quantum simulation hereafter) of any many-body fermionic Hamiltonian. We show how to generate, via various Jordan-Wigner transformations, all qubit operations needed to simulate the time evolution operator of a given Hamiltonian. We also show that for a given term in an m-body fermionic Hamiltonian, the number of operations needed to simulate it is linear in the number of qubits or energy-levels of the system. The number of terms in the Hamiltonian is of the order of m^2 for a general m-body interaction, making the simulation increasingly harder with higher order interactions. We specialize our examples to a two-body Hamiltonian, since this is also the most general type of Hamiltonian encountered in many-body physics. Besides fields like nuclear physics, where three-body forces play a non-neglible role, a two-body Hamiltonian captures most of the relevant physics. The various transformations are detailed in the next section. In Sec. III we show in detail how to simulate a quantum computer finding the eigenvalues of any two-body Hamiltonian, with all available particle numbers, using the simulated time evolution operator. In that section we describe also the techniques which are necessary for the extraction of information using a phase-estimation

algorithm.

To demonstrate the feasibility of our algorithm, we present in Sec. IV selected results from applications of our algorithm to two simple model-Hamiltonians, a pairing Hamiltonian and the Hubbard model. We summarize our results and present future perspectives in Sec. V.

II. ALGORITHM FOR QUANTUM COMPUTATIONS OF FERMIONIC SYSTEMS

A.   Hamiltonians

A general two-body Hamiltonian for fermionic system can be written as

$$H = E_0 + \sum_{ij=1} E_{ij} a_i^\dagger a_j + \sum_{ijkl=1} V_{ijkl} a_i^\dagger a_j^\dagger a_l a_k, \qquad (1)$$

where E_0 is a constant energy term, E_{ij} represent all the one-particle terms, allowing for non-diagonal terms as well. The one-body term can represent a chosen single-particle potential, the kinetic energy or other more specialized terms such as those discussed in connection with the Hubbard model [29] or the pairing Hamiltonian discussed below. The two-body interaction part is given by V_{ijkl} and can be any two-body interaction, from Coulomb interaction to the interaction between nucleons. The sums run over all possible single-particle levels N. Note that this model includes particle numbers from zero to the number of available quantum levels, n. To simulate states with fixed numbers of fermions one would have to either rewrite the Hamiltonian or generate specialized input states in the simulation.

The algorithm which we will develop in this section and in Sec. III can treat any two-body Hamiltonian. However, in our demonstrations of the quantum computing algorithm, we will limit ourselves to two simple models, which however capture much of the important physics in quantum mechanical many-body systems. We will also limit ourselves to spin $j = 1/2$ systems, although our algorithm can also simulate higher j-values, such as those which occur in nuclear, atomic and molecular physics, it simply uses one qubit for every available quantum state. These simple models are the Hubbard model and a pairing Hamiltonian. We start with the spin 1/2 Hubbard model, described by the following Hamiltonian

$$\begin{aligned} H_H \quad &= \epsilon \sum_{i,\sigma} a_{i\sigma}^\dagger a_{i\sigma} - t \sum_{i,\sigma} \left(a_{i+1,\sigma}^\dagger a_{i,\sigma} + a_{i,\sigma}^\dagger a_{i+1,\sigma} \right) \\ &+ U \sum_{i=1} a_{i+}^\dagger a_{i-}^\dagger a_{i-} a_{i+}, \end{aligned} \qquad (2)$$

where $a^\dagger$ and a are fermion creation and annihilation operators, respectively. This is a chain of sites where each site has room for one spin up fermion and one spin down fermion. The number of sites is N, and the sums over σ are sums over spin up and down only. Each site

has a single-particle energy ϵ. There is a repulsive term U if there is a pair of particles at the same site. It is energetically favourable to tunnel to neighbouring sites, described by the hopping terms with coupling constant $-t$.

The second model-Hamiltonian is the simple pairing Hamiltonian

$$H_P = \sum_i \varepsilon_i a_i^\dagger a_i - \frac{1}{2} g \sum_{ij>0} a_i^\dagger a_{\bar{\imath}}^\dagger a_{\bar{\jmath}} a_j, \qquad (3)$$

The indices i and j run over the number of levels N, and the label $\bar{\imath}$ stands for a time-reversed state. The parameter g is the strength of the pairing force while ε_i is the single-particle energy of level i. In our case we assume that the single-particle levels are equidistant (or degenerate) with a fixed spacing d. Moreover, in our simple model, the degeneracy of the single-particle levels is set to $2j + 1 = 2$, with $j = 1/2$ being the spin of the particle. This gives a set of single-particle states with the same spin projections as for the Hubbard model. Whereas in the Hubbard model we operate with different sites with spin up or spin down particles, our pairing models deals thus with levels with double degeneracy. Introducing the pair-creation operator $S_i^+ = a_{im}^\dagger a_{i-m}^\dagger$, one can rewrite the Hamiltonian in Eq. (3) as

$$H_P = d \sum_i i N_i + \frac{1}{2} G \sum_{ij>0} S_i^+ S_j^-,$$

where $N_i = a_i^\dagger a_i$ is the number operator, and $\varepsilon_i = id$ so that the single-particle orbitals are equally spaced at intervals d. The latter commutes with the Hamiltonian H. In this model, quantum numbers like seniority $\mathcal{S}$ are good quantum numbers, and the eigenvalue problem can be rewritten in terms of blocks with good seniority. Loosely speaking, the seniority quantum number $\mathcal{S}$ is equal to the number of unpaired particles; see [30] for further details. Furthermore, in a series of papers, Richardson, see for example Refs. [31, 32, 33], obtained the exact solution of the pairing Hamiltonian, with semi-analytic (since there is still the need for a numerical solution) expressions for the eigenvalues and eigenvectors. The exact solutions have had important consequences for several fields, from Bose condensates to nuclear superconductivity and is currently a very active field of studies, see for example Refs. [34, 35]. Finally, for particle numbers up to $P \sim 20$, the above model can be solved exactly through numerical diagonalization and one can obtain all eigenvalues. It serves therefore also as an excellent ground for comparison with our algorithm based on models from quantum computing.

B.   Basic quantum gates

Benioff showed that one could make a quantum mechanical Turing machine by using various unitary opera-

tions on a quantum system, see Ref. [36]. Benioff demonstrated that a quantum computer can calculate anything a classical computer can. To do this one needs a quantum system and basic operations that can approximate all unitary operations on the chosen many-body system. We describe in this subsection the basic ingredients entering our algorithms.

1. Qubits, gates and circuits

In this article we will use the standard model of quantum information, where the basic unit of information is the qubit, the quantum bit. As mentioned in the introduction, any suitable two-level quantum system can be a qubit, it is the smallest system there is with the least complex dynamics. Qubits are both abstract measures of information and physical objects. Actual physical qubits can be ions trapped in magnetic fields where lasers can access only two energy levels or the nuclear spins of some of the atoms in molecules accessed and manipulated by an NMR machine. Several other ideas have been proposed and some tested, see [37].

The computational basis for one qubit is $|0\rangle$ (representing for example bit 0) for the first state and $|1\rangle$ (representing bit 1) for the second, and for a set of qubits the tensor products of these basis states for each qubit form a product basis. Below we write out the different basis states for a system of n qubits.

$$
\begin{aligned}
|0\rangle &\equiv |00\cdots 0\rangle = |0\rangle \otimes |0\rangle \otimes \cdots \otimes |0\rangle \\
|1\rangle &\equiv |00\cdots 1\rangle = |0\rangle \otimes |0\rangle \otimes \cdots \otimes |1\rangle \\
&\quad\quad\quad\quad\quad \vdots \\
|2^n - 1\rangle &\equiv |11\cdots 1\rangle = |1\rangle \otimes |1\rangle \otimes \cdots \otimes |1\rangle.
\end{aligned}
\tag{4}
$$

This is a 2^n-dimensional system and we number the different basis states using binary numbers corresponding to the order in which they appear in the tensor product.

Quantum computing means to manipulate and measure qubits in such a way that the results from a measurement yield the solutions to a given problem. The quantum operations we need to be able to perform our simulations are a small set of elementary single-qubit operations, or single-qubit gates, and one universal two-qubit gate, in our case the so-called CNOT gate defined below.

To represent quantum computer algorithms graphically we use circuit diagrams. In a circuit diagram each qubit is represented by a line, and operations on the different qubits are represented by boxes. In fig. 1 we show an example of a quantum circuit, with the arrow indicating the time evolution, The states $|a\rangle$ and $|b\rangle$ in the figure represent qubit states. In general, the total state will be a superposition of different qubit states. A single-qubit gate is an operation that only affects one physical qubit, for example one ion or one nuclear spin in a molecule. It
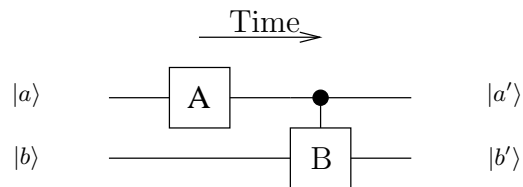

FIG. 1: A quantum circuit showing a single-qubit gate A and a two-qubit gate acting on a pair of qubits, represented by the horizontal lines.

is represented by a box on the line corresponding to the qubit in question. A single-qubit gate operates on one qubit and is therefore represented mathematically by a 2×2 matrix while a two-qubit gate is represented by a 4×4 matrix. As an example we can portray the so-called CNOT gate as matrix,

$$
\begin{pmatrix}
1 & 0 & 0 & 0 \\
0 & 1 & 0 & 0 \\
0 & 0 & 0 & 1 \\
0 & 0 & 1 & 0
\end{pmatrix}.
\tag{5}
$$

This is a very important gate, since one can show that it behaves as a universal two-qubit gate, and that we only need this two-qubit gate and a small set of single-qubit gates to be able to approximate any multi-qubit operation. One example of a universal set of single-qubit gates is given in Fig. 2. The products of these three operations on one qubit can approximate to an arbitrary precision any unitary operation on that qubit.
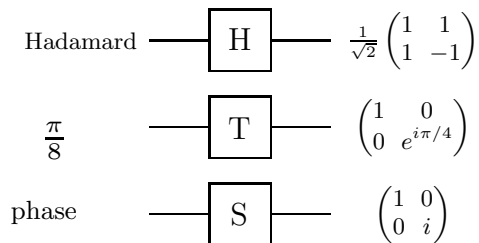

FIG. 2: Set of three elementary single-qubit gates and their matrix representations. The products of these three operations on one qubit can approximate to an arbitrary precision any unitary operation on that qubit.

2. Decomposing unitary operations into gates

The next step is to find elementary operations on a set of qubits that can be put together in order to approximate any unitary operation on the qubits. In this way we can perform computations on a quantum computer by performing many of these elementary operations in the correct order.

There are three steps in finding the elementary operations needed to simulate any unitary operation. First,

any $d \times d$ unitary matrix can be factorized into a product of at most $d(d-1)/2$ two-level unitary matrices, see for example Ref. [37] for details. A two-level unitary matrix is a matrix that only acts non-trivially on two vector components when multiplied with a vector. For all other vector components it acts as the identity operation.

The next step is to prove that any two-level unitary matrix can be implemented by one kind of two-qubit gate, for example the CNOT gate in Eq. (5), and single-qubit gates only. This simplifies the making of actual quantum computers as we only need one type of interaction between pairs of qubits. All other operations are operations on one qubit at the time.

Finally, these single-qubit operations can be approximated to an arbitrary precision by a finite set of single-qubit gates. Such a set is called a universal set and one example is the phase gate, the so-called Hadamard gate and the $\pi/8$ gate. Fig. 2 shows these gates. By combining these properly with the CNOT gate one can approximate any unitary operation on a set of qubits.

3. Quantum calculations

The aspect of quantum computers we are focusing on in this article is their use in computing properties of quantum systems. When we want to use a quantum computer to find the energy levels of a quantum system or simulate it's dynamics, we need to simulate the time evolution operator of the Hamiltonian, $U = \exp(-iH\Delta t)$. To do that on a quantum computer we must find a set of single- and two-qubit gates that would implement the time evolution on a set of qubits. For example, if we have one qubit in the state $|a\rangle$, we must find the single-qubit gates that when applied results in the qubit being in the state $\exp(-iH\Delta t)|a\rangle$.

From what we have written so far the naive way of simulating U would be to calculate it directly as a matrix in an appropriate basis, factorize it into two-level unitary matrices and then implement these by a set of universal gates. In a many-body fermion system for example, one could use the Fock basis to calculate U as a matrix. A fermion system with n different quantum levels can have from zero to n particles in each Fock basis state. A two-level system has four different basis states, $|00\rangle$, $|01\rangle$, $|10\rangle$ and $|11\rangle$, where $|0\rangle$ corresponds to an occupied quantum level. The time evolution matrix is then a $2^n \times 2^n$ matrix. This matrix is then factorized into at most $2^n(2^n-1)/2$ two-level unitary matrices. An exponential amount of operations, in terms of the number of quantum levels, is needed to simulate U; by definition not an effective simulation.

This shows that quantum computers performing quantum simulations not necessarily fulfill their promise. For each physical system to be simulated one has to find representations of the Hamiltonian that leads to polynomial complexity in the number of operations. After one has found a proper representation of the Hamiltonian, the time evolution operator $\exp(-iH\Delta t)$ is found by using a Trotter approximation, for example

$$U = e^{-iH\Delta t} = e^{-i(\sum_k H_k)\Delta t} = \prod_k e^{-iH_k \Delta t} + \mathcal{O}(\Delta t^2).$$
(6)

There are different ways to approximate U by products of exponentials of the different terms of the Hamiltonian, see Ref. [37] and Eq. (41). The essential idea is to find a form of the Hamiltonian where these factors in the approximated time evolution operator can be further factorized into single- and two-qubit operations effectively. In Refs. [24, 38] it was shown how to do this in principle for any many-body fermion system using the Jordan-Wigner transformation. In this article we show how to create a quantum compiler that takes any many-body fermion Hamiltonian and outputs the quantum gates needed to simulate the time evolution operator. We implement it for the case of two-body fermion Hamiltonians and show results from numerical calculations finding the energylevels of the well known pairing and Hubbard models.

C. The Jordan-Wigner transformation

For a spin-1/2 one-dimensional quantum spin-chain a fermionization procedure exists which allows the mapping between spin operators and fermionic creation-annihilation operators. The algebra governing the spin chain is the $SU(2)$ algebra, represented by the σ-matrices. The Jordan-Wigner transformation is a transformation from fermionic annihilation and creation operators to the σ-matrices of a spin-1/2 chain, see for example Ref. [39] for more details on the Jordan-Wigner transformation.

There is an isomorphism between the two systems, meaning that any a or $a^\dagger$ operator can be transformed into a tensor product of σ-matrices operating on a set of qubits. This was explored by Somma *et al.* in Refs. [24, 25]. The authors demonstrated, with an emphasis on single-particle fermionic operators, that the Jordan-Wigner transformation ensures efficient, i.e., not exponential complexity, simulations of a fermionic system on a quantum computer. Similar transformations must be found for other systems, in order to efficiently simulate many-body systems. This was the main point in Ref. [25].

We present here the various ingredients needed in order to transform a given Hamiltonian into a practical form suitable for quantum mechanical simulations.

We begin with the fermionic creation and annihilation operators, which satisfy the following anticommutation relations

$$\{a_k, a_l\} = \{a_k^\dagger, a_l^\dagger\} = 0, \quad \{a_k^\dagger, a_l\} = \delta_{kl}.$$
(7)

Thereafter we define the three traceless and Hermitian generators of the $SU(2)$ group, the σ-matrices σ_x, σ_y and σ_z. Together with the identity matrix $\mathbf{1}$ they form

a complete basis for all Hermitian 2×2 matrices. They can be used to write all Hamiltonians on a spin 1/2 chain when taking sums of tensor products of these, in other words they form a product basis for the operators on the qubits. The three σ-matrices are

$$\sigma_x = \begin{pmatrix} 0 & 1 \\ 1 & 0 \end{pmatrix}, \sigma_y = \begin{pmatrix} 0 & -i \\ i & 0 \end{pmatrix}, \quad \sigma_z = \begin{pmatrix} 1 & 0 \\ 0 & -1 \end{pmatrix}. \quad (8)$$

We define the raising and lowering matrices as

$$\sigma_+ = \frac{1}{2}(\sigma_x + i\sigma_y) = \begin{pmatrix} 0 & 1 \\ 0 & 0 \end{pmatrix},$$

$$\sigma_- = \frac{1}{2}(\sigma_x - i\sigma_y) = \begin{pmatrix} 0 & 0 \\ 1 & 0 \end{pmatrix}. \quad (9)$$

The transformation is based on the fact that for each possible quantum state of the fermion system, there can be either one or zero fermions. Therefore we need n qubits for a system with n possible fermion states. A qubit in state $|0\rangle^i = a_i^\dagger |vacuum\rangle$ represents a state with a fermion, while $|1\rangle^i = |vacuum\rangle$ represents no fermions. Then the raising operator σ_+ changes $|1\rangle$ into $|0\rangle$ when

$$|0\rangle \equiv \begin{pmatrix} 1 \\ 0 \end{pmatrix}, \quad |1\rangle \equiv \begin{pmatrix} 0 \\ 1 \end{pmatrix}. \quad (10)$$

This means that σ_+ acts as a creation operator, and σ_- acts as an annihilation operator. In addition, because of the anticommutation of creation(annihilation) operators for different states we have $a_1^\dagger a_2^\dagger |vacuum\rangle = -a_2^\dagger a_1^\dagger |vacuum\rangle$, meaning that for creation and annihilation operators for states higher than the state corresponding to the first qubit, we need to multiply with a σ_z-matrix on all the qubits leading up to the one in question, in order to get the correct sign in the final operation. This leads us to the Jordan-Wigner transformation [24, 25]

$$a_n^\dagger = \left(\prod_{k=1}^{n-1} \sigma_z^k\right) \sigma_+^n, \quad a_n = \left(\prod_{k=1}^{n-1} \sigma_z^k\right) \sigma_-^n. \quad (11)$$

The notation $\sigma_z^i \sigma_+^j$ means a tensor product of the identity matrix on all qubits other than i and j, $\mathbf{1} \otimes \sigma_z \otimes \mathbf{1} \otimes \sigma_+ \otimes \mathbf{1}$, if $i < j$, with $\mathbf{1}$ being the identity matrices of appropriate dimension.

D. Single-particle Hamiltonian

What we must do now is to apply the Jordan-Wigner transformation to a general fermionic Hamiltonian composed of creation and annihilation operators, so we can write it as a sum of products of σ matrices. The matrix σ^k is then an operation on the kth qubit representing the

k^{th} quantum level of the fermion system. When we have expressed the Hamiltonian as a sum of products of operations on the qubits representing the system, we must find a representation of the time evolution operator as products of two-qubit operations. These operations can be further decomposed into elementary operations, see subsection II B 1 for further discussion.

1. Jordan-Wigner transformation of the one-body part

We first describe the procedure for the simplest case of a general single-particle Hamiltonian,

$$H_1 = \sum_i E_{ii} a_i^\dagger a_i + \sum_{i<j} E_{ij}(a_i^\dagger a_j + a_j^\dagger a_i). \quad (12)$$

We now use the transformation of Eq. (11) on the terms $a_i^\dagger a_j$.

The diagonal terms of the one-particle Hamiltonian, that is the case where $i = j$, can be rewritten as

$$a_i^\dagger a_i = \left(\prod_{k=1}^{i-1} \sigma_z^k\right) \sigma_+^i \left(\prod_{k=1}^{i-1} \sigma_z^k\right) \sigma_-^i$$

$$= \sigma_+^i \sigma_-^i = \frac{1}{2}\left(\mathbf{1}^i + \sigma_z^i\right), \quad (13)$$

since $(\sigma_z)^2 = \mathbf{1}$ which is the number operator. It counts whether or not a fermion is in state i. In the case of qubits counting whether or not the qubit is in state $|0\rangle$, we have eigenvalue one for $|0\rangle$ and eigenvalue zero for $|1\rangle$. The action of this Hamiltonian on qubit i can be simulated using the single-qubit operation

$$U = e^{-i(\mathbf{1}+\sigma_z)E_{ii}\Delta t} = \begin{pmatrix} e^{-iE_{ii}\Delta t} & 0 \\ 0 & 1 \end{pmatrix}, \quad (14)$$

see subsection II B 1 for other examples of single-qubit gates.

For the non-diagonal elements, $i < j$, not all of the σ_z matrices multiply with each other and end up in the identity operation. As an example we will consider a five level system, $n = 5$, and look at the transformation of the term $a_i^\dagger a_j$ whith $i = 2$ and $j = 4$,

$$\begin{aligned} a_2^\dagger &= \sigma_z \otimes \sigma_+ \otimes \mathbf{1} \otimes \mathbf{1} \otimes \mathbf{1}, \\ a_4 &= \sigma_z \otimes \sigma_z \otimes \sigma_z \otimes \sigma_- \otimes \mathbf{1}, \\ &\Downarrow \\ a_2^\dagger a_4 &= \mathbf{1} \otimes (\sigma_+ \sigma_z) \otimes \sigma_z \otimes \sigma_- \otimes \mathbf{1}. \quad (15) \end{aligned}$$

The operation on all qubits before i and after j is identity, on qubits $i+1$ through $j-1$ it is σ_z. We can then write the non-diagonal one-body operators as

$$a_i^\dagger a_j + a_j^\dagger a_i \quad = (\sigma_+^i \sigma_z^i) \left(\prod_{k=i+1}^{j-1} \sigma_z^k \right) \sigma_-^j + (\sigma_z^i \sigma_-^i) \left(\prod_{k=i+1}^{j-1} \sigma_z^k \right) \sigma_+^j$$

$$= -\sigma_+^i \left(\prod_{k=i+1}^{j-1} \sigma_z^k \right) \sigma_-^j - \sigma_-^i \left(\prod_{k=i+1}^{j-1} \sigma_z^k \right) \sigma_+^j$$

$$= -\frac{1}{2} \left\{ \sigma_x^i \left(\prod_{k=i+1}^{j-1} \sigma_z^k \right) \sigma_x^j + \sigma_y^i \left(\prod_{k=i+1}^{j-1} \sigma_z^k \right) \sigma_y^j \right\}. \tag{16}$$

Using Eqs. (13) and (16) the total single-particle fermionic Hamiltonian of n quantum levels, transformed using the Jordan-Wigner transformation of Eq. (11), is written as

$$H_1 = \sum_i E_{ii} a_i^\dagger a_i + \sum_{i<j} E_{ij} (a_i^\dagger a_j + a_j^\dagger a_i)$$

$$= \frac{1}{2} \sum_i E_{ii} \left(\mathbf{1}^i + \sigma_z^i \right)$$

$$- \frac{1}{2} \sum_{i<j} E_{ij} \left\{ \sigma_x^i \left(\prod_{k=i+1}^{j-1} \sigma_z^k \right) \sigma_x^j \right.$$

$$+ \left. \sigma_y^i \left(\prod_{k=i+1}^{j-1} \sigma_z^k \right) \sigma_y^j \right\}. \tag{17}$$

2. Transformation into two-qubit operations

The Hamiltonian is now transformed into a sum of many-qubit operations, $H = \sum_l H_l$. The $a_2^\dagger a_4$ term in Eq. (15) for example, is transformed into a three-qubit operation. The next step is to factorize these many-qubit operations H_l into products of two-qubit operations, so that we in the end can get a product of two-qubit operations U_{kl}, that when performed in order give us the time evolution operator corresponding to each term in the Hamiltonian, $\exp(-iH_l\Delta t) = \prod_k U_{kl}$.

The first thing we do is to find a set of two-qubit operations that together give us the Hamiltonian, and later we will see that to find the time evolution from there is straightforward. The many-qubit terms in Eq. (17) are products of the type $\sigma_x \sigma_z \cdots \sigma_z \sigma_x$ with σ_x or σ_y at either end. These products have to be factorized into a series of two-qubit operations. What we wish to do is successively build up the operator using different unitary transformations. This can be achieved with successive operations with the σ-matrices, starting with for example σ_z^i, which can be transformed into σ_x^i, then transformed into $\sigma_y^i \sigma_z^{i+1}$ and so forth. Our goal now is to express each term in the Hamiltonian Eq. (17) as a product of the type $\sigma_x^i \sigma_z \cdots \sigma_z \sigma_x^j = (\prod_k U_k^\dagger) \sigma_z^i (\prod_{k'} U_{k'})$, with a different form in the case where the Hamiltonian term starts and ends with a σ_y matrix. To achieve this we need the

transformations in Eqs. (A.8)-(A.11). We will use this to find the time-evolution operator for each Hamiltonian, see Eq. (21) below.

To understand how we factorize the Hamiltonian terms into single- and two-qubit operations we follow a bottom up procedure. First, if we have a two qubit system, with the operator $\sigma_z \otimes \mathbf{1}$, we see that the unitary operation $\exp(i\pi/4\sigma_z \otimes \sigma_z)$ transforms it into

$$e^{-i\pi/4\sigma_z \otimes \sigma_z} (\sigma_z \otimes \mathbf{1}) e^{i\pi/4\sigma_z \otimes \sigma_z} = \sigma_z \otimes \sigma_z. \tag{18}$$

In addition, if we start out with the operator σ_z^i we can transform it into σ_x^i or σ_y^i using the operators $\exp(i\pi/4\sigma_y)$ or $\exp(-i\pi/4\sigma_x)$ accordingly.

We can then generate the $\prod_k \sigma_z^k$ part of the terms in Eq. (17) by succesively applying the operator $\exp(i\pi/4\sigma_z^i \sigma_z^l)$ for $l = 2$ through $l = j$. Yielding the operator $\sigma_a^i \prod_{k=i+1}^j \sigma_z^k$ with a phase of ± 1, because of the sign change in Eqs. (A.10) and (A.11). We write σ_a to show that we can start with both a σ_x and a σ_y matrix. To avoid the sign change we can simply use the operator $\exp(-i\pi/4\sigma_z^i \sigma_z^l)$ instead for those cases where we have σ_y^i on site i instead of σ_x^i. This way we always keep the same phase.

Finally, we use the operator $\exp(i\pi/4\sigma_y)$ if we want the string of operators to end with σ_x, or $\exp(-i\pi/4\sigma_x)$ if we want it to end with σ_y. The string of operators starts with either σ_x or σ_y. For an odd number of $\exp(\pm i\pi/4\sigma_z^i \sigma_z^l)$ operations, the operations that add a σ_z to the string, the first operator has changed from what we started with. In other words we have σ_x instead of σ_y at the start of the string or vice versa, see Eqs. (A.10) and (A.11). By counting, we see that we do $j - i$ of the $\exp(\pm i\pi/4\sigma_z^i \sigma_z^l)$ operations to get the string $\sigma_a^i \sigma_z^{i+1} \cdots \sigma_z^j$. and therefore if $j-i$ is odd, the first matrix is the opposite of what we want in the final string. The following simple example can serve to clarify. We want the Hamiltonian $\sigma_x^1 \sigma_z^2 \sigma_x^3 = \sigma_x \otimes \sigma_z \otimes \sigma_x$, and by using the transformations in Eqs. (A.8)-(A.11) we can construct it as a product of single- and two-qubit operations in the

following way,

$$
\begin{aligned}
(e^{-\pi/4\sigma_y^1})\sigma_z^1(e^{\pi/4\sigma_y^1}) &= \sigma_x^1 \\
(e^{-i\pi/4\sigma_z^1\sigma_z^2})\sigma_x^1(e^{i\pi/4\sigma_z^1\sigma_z^2}) &= \sigma_y^1\sigma_z^2 \\
(e^{i\pi/4\sigma_z^1\sigma_z^3})\sigma_y^1\sigma_z^2(e^{-i\pi/4\sigma_z^1\sigma_z^3}) &= \sigma_x^1\sigma_z^2\sigma_z^3 \\
(e^{-i\pi/4\sigma_y^3})\sigma_x^1\sigma_z^2\sigma_z^3(e^{i\pi/4\sigma_y^3}) &= \sigma_x^1\sigma_z^2\sigma_x^3.
\end{aligned}
\quad (19)
$$

We see that we have factorized $\sigma_x^1\sigma_z^2\sigma_x^3$ into $U_4^\dagger U_3^\dagger U_2^\dagger U_1^\dagger \sigma_z^1 U_1 U_2 U_3 U_4$.

Now we can find the time-evolution operator $\exp(-iH\Delta t)$ corresponding to each term of the Hamiltonian, which is the quantity of interest. Instead of starting with the operator σ_z^i we start with the corresponding evolution operator and observe that

$$
\begin{aligned}
U^\dagger e^{-i\sigma_z a} U &= U^\dagger \left(\cos(a)\mathbf{1} - i\sin(a)\sigma_z\right) U \\
&= \cos(a)\mathbf{1} - i\sin(a)U^\dagger\sigma_z U \\
&= e^{-iU^\dagger\sigma_z U a},
\end{aligned}
\quad (20)
$$

where a is a scalar. This means that we have a series of unitary transformations on this operator yielding the final evolution, namely

$$
e^{-i\sigma_x^i\sigma_z\cdots\sigma_z\sigma_x^j a} = \left(\prod_k U_k^\dagger\right) e^{-i\sigma_z^i a}\left(\prod_{k'} U_{k'}\right),
\quad (21)
$$

with the exact same unitary operations U_k as we find when we factorize the Hamiltonian. These are now the single- and two-qubit operations we were looking for, first we apply the operations U_k to the appropriate qubits, then $\exp(-i\sigma_z^i a)$ to qubit i, and then the $U_k^\dagger$ operations, all in usual matrix multiplication order.

E. Two-body Hamiltonian

In this section we will do the same for the general two-body fermionic Hamiltonian. The two-body part of the Hamiltonian can be classified into diagonal elements and non-diagonal elements. Because of the Pauli principle and the anti-commutation relations for the creation and annihilation operators, some combinations of indices are not allowed. The two-body part of our Hamiltonian is

$$
H_2 = \sum_{ijkl} V_{ijkl} a_i^\dagger a_j^\dagger a_l a_k,
\quad (22)
$$

where the indices run over all possible states and n is the total number of available quantum states. The single-particle labels $ijkl$ refer to their corresponding sets of quantum numbers, such as projection of total spin, number of nodes in the single-particle wave function etc. Since every state $ijkl$ is uniquely defined, we cannot have two equal creation or annihilation operators and therefore $i \neq j$ and $k \neq l$.

When $i = l$ and $j = k$, or $i = k$ and $j = l$, we have a diagonal element in the Hamiltonian matrix, and the output state is the same as the input state. The operator term corresponding to V_{ijji} has these equalities due to the anti-commutation relations

$$
\begin{aligned}
a_i^\dagger a_j^\dagger a_i a_j &= a_j^\dagger a_i^\dagger a_j a_i \\
&= -a_i^\dagger a_j^\dagger a_j a_i \\
&= -a_j^\dagger a_i^\dagger a_i a_j,
\end{aligned}
\quad (23)
$$

which means that

$$
V_{ijji} = V_{jiij} = -V_{ijij} = -V_{jiji}.
\quad (24)
$$

The term $a_i^\dagger a_j^\dagger a_i a_j$ with $i < j$ is described using the Pauli matrices

$$
a_i^\dagger a_j^\dagger a_i a_j \qquad\qquad\qquad\qquad (25)
$$
$$
\begin{aligned}
&= \left(\prod_{s=1}^{i-1}\sigma_z\right)\sigma_+^i\left(\prod_{t=1}^{j-i}\sigma_z\right)\sigma_+^j \\
&\times \left(\prod_{t=1}^{j-i}\sigma_z\right)\sigma_-^j\left(\prod_{s=1}^{i-1}\sigma_z\right)\sigma_-^i \\
&= \left(\prod_{s=1}^{i-1}(\sigma_z)^4\right)\left(\sigma_+^i\sigma_z^i\sigma_z^i\sigma_-^i\right)\left(\prod_{t=i+1}^{j-1}(\sigma_z)^2\right)\left(\sigma_+^j\sigma_-^j\right) \\
&= \sigma_+^i\sigma_-^i\sigma_+^j\sigma_-^j \\
&= \frac{1}{16}\left(\mathbf{1}+\sigma_z^i\right)\left(\mathbf{1}+\sigma_z^j\right).
\end{aligned}
\quad (26)
$$

When we add all four different permutations of i and j this is the number operator on qubit i multiplied with the number operator on qubit j. The eigenvalue is one if both qubits are in the state $|0\rangle$, that is the corresponding quantum states are both populated, and zero otherwise. We can in turn rewrite the sets of creation and annihilations in terms of the σ-matrices as

$$
a_i^\dagger a_j^\dagger a_i a_j + a_j^\dagger a_i^\dagger a_j a_i - a_i^\dagger a_j^\dagger a_j a_i - a_j^\dagger a_i^\dagger a_i a_j
$$
$$
= \frac{1}{4}\left(\mathbf{1}+\sigma_z^i+\sigma_z^j+\sigma_z^i\sigma_z^j\right).
\quad (27)
$$

In the general case we can have three different sets of non-equal indices. Firstly, we see that $a_i^\dagger a_j^\dagger a_l a_k = a_k^\dagger a_l^\dagger a_j a_i$, meaning that the exchange of i with k and j with l gives the same operator $\rightarrow V_{ijkl} = V_{klij}$. This results in a two-body Hamiltonian with no equal indices

$$
H_{ijkl} = \sum_{i<k}\sum_{j<l} V_{ijkl}(a_i^\dagger a_j^\dagger a_l a_k + a_k^\dagger a_l^\dagger a_j a_i).
\quad (28)
$$

Choosing to order the indices from lowest to highest gives us the position where there will be σ_z-matrices to multiply with the different raising and lowering operators, when we perform the Jordan-Wigner transformation Eq. (11). The order of matrix multiplications is fixed once and for all, resulting in three different groups into which these terms fall, namely

$$
\begin{array}{llll}
I & i<j<l<k, & i\leftrightarrow j, & k\leftrightarrow l, \\
II & i<l<j<k, & i\leftrightarrow j, & k\leftrightarrow l, \\
III & i<l<k<j, & i\leftrightarrow j, & k\leftrightarrow l.
\end{array}
\quad (29)
$$

These 12 possibilities for $a_i^\dagger a_j^\dagger a_l a_k$ are mirrored in the symmetric term in Eq. (28) giving us the 24 different possibilities when permuting four indices.

The $ijkl$ term of Eq. (28) is

$$a_i^\dagger a_j^\dagger a_l a_k + a_k^\dagger a_l^\dagger a_j a_i =$$
$$\left(\prod \sigma_z\right)\sigma_+^i \left(\prod \sigma_z\right)\sigma_+^j$$
$$\times \left(\prod \sigma_z\right)\sigma_-^l \left(\prod \sigma_z\right)\sigma_-^k$$
$$+ \left(\prod \sigma_z\right)\sigma_+^k \left(\prod \sigma_z\right)\sigma_+^l$$
$$\times \left(\prod \sigma_z\right)\sigma_-^j \left(\prod \sigma_z\right)\sigma_-^i. \tag{30}$$

In the case of $i < j < l < k$ we have

$$a_i^\dagger a_j^\dagger a_l a_k + a_k^\dagger a_l^\dagger a_j a_i =$$
$$\left(\prod (\sigma_z)^4\right)(\sigma_+^i \sigma_z^i)\left(\prod (\sigma_z)^3\right)\sigma_+^j$$
$$\times \left(\prod (\sigma_z)^2\right)(\sigma_-^l \sigma_z^l)\left(\prod \sigma_z\right)\sigma_-^k$$
$$+ \left(\prod (\sigma_z)^4\right)(\sigma_z^i \sigma_-^i)\left(\prod (\sigma_z)^3\right)\sigma_-^j$$
$$\times \left(\prod (\sigma_z)^2\right)(\sigma_z^l \sigma_+^l)\left(\prod \sigma_z\right)\sigma_+^k. \tag{31}$$

Using Eq. (A.12), where we have the rules for sign changes when multiplying the raising and lowering operators with the σ_z matrices, gives us

$$-\left(\sigma_+^i \sigma_z^{i+1}\cdots\sigma_z^{j-1}\sigma_+^j \sigma_-^l \sigma_z^{l+1}\cdots\sigma_z^{k-1}\sigma_-^k \right.$$
$$\left. + \sigma_-^i \sigma_z^{i+1}\cdots\sigma_z^{j-1}\sigma_-^j \sigma_+^l \sigma_z^{l+1}\cdots\sigma_z^{k-1}\sigma_+^k \right). \tag{32}$$

If we switch the order of i and j so that $j < i < l < k$, we change the order in which the σ_z-matrix is multiplied with the first raising and lowering matrices, resulting in a sign change.

$$a_i^\dagger a_j^\dagger a_l a_k + a_k^\dagger a_l^\dagger a_j a_i =$$
$$\left(\prod (\sigma_z)^4\right)(\sigma_z^j \sigma_+^j)\left(\prod (\sigma_z)^3\right)\sigma_+^i$$
$$\times \left(\prod (\sigma_z)^2\right)(\sigma_-^l \sigma_z^l)\left(\prod \sigma_z\right)\sigma_-^k$$
$$+ \left(\prod (\sigma_z)^4\right)(\sigma_-^j \sigma_z^j)\left(\prod (\sigma_z)^3\right)\sigma_-^i$$
$$\times \left(\prod (\sigma_z)^2\right)(\sigma_z^l \sigma_+^l)\left(\prod \sigma_z\right)\sigma_+^k$$
$$= +\left(\sigma_+^j \sigma_z^{j+1}\cdots\sigma_z^{i-1}\sigma_+^i \sigma_-^l \sigma_z^{l+1}\cdots\sigma_z^{k-1}\sigma_-^k \right.$$
$$\left. + \sigma_-^j \sigma_z^{j+1}\cdots\sigma_z^{i-1}\sigma_-^i \sigma_+^l \sigma_z^{l+1}\cdots\sigma_z^{k-1}\sigma_+^k \right). \tag{33}$$

We get a change in sign for every permutation of the ordering of the indices from lowest to highest because of the matrix multiplication ordering. The ordering is described by another set of indices $\{s_\alpha, s_\beta, s_\gamma, s_\delta\} \in \{i, j, k, l\}$ where $s_\alpha < s_\beta < s_\gamma < s_\delta$. We assign a number to each of the four indices, $i \leftrightarrow 1$,

$j \leftrightarrow 2$, $l \leftrightarrow 3$ and $k \leftrightarrow 4$. If $i < j < l < k$ we say the ordering is $\alpha = 1$, $\beta = 2$, $\gamma = 3$ and $\delta = 4$, where α is a number from one to four indicating which of the indices i, j, l and k is the smallest. If i is the smallest, $\alpha = 1$ and $s_\alpha = i$. This allows us to give the sign of a given $(a_i^\dagger a_j^\dagger a_l a_k + a_k^\dagger a_l^\dagger a_j a_i)$ term using the totally anti-symmetric tensor with four indices, which is $+1$ for even permutations, and -1 for odd permutations. For each of the three groups in Eq. (29) we get a different set of raising and lowering operators on the lowest, next lowest and so on, indices, while the sign for the whole set is given by $-\varepsilon^{\alpha\beta\gamma\delta}$.

We are in the position where we can use the relation in Eq. (9) to express the Hamiltonian in terms of the σ-matrices. We get 16 terms with products of four σ_x and or σ_y matrices in the first part of Eq. (31), then when we add the Hermitian conjugate we get another 16 terms. The terms with an odd number of σ_y matrices have an imaginary phase and are therefore cancelled out when adding the conjugates in Eq. (28). This leaves us with just the terms with four σ_x matrices, four σ_y matrices and two of each in different orderings. The final result is given as an array with a global sign and factor given by the permutation of the ordering, and eight terms with different signs depending on which of the three groups, Eq. (29), the set of indices belong to. These differing rules are due to the rules for σ_z multiplication with the raising and lowering operators, resulting in

$$a_i^\dagger a_j^\dagger a_l a_k + a_k^\dagger a_l^\dagger a_j a_i =$$

$$-\frac{\varepsilon^{\alpha\beta\gamma\delta}}{8}\begin{cases} I & II & III \\ + & + & + & \sigma_x^{s_\alpha}\sigma_z\cdots\sigma_z\sigma_x^{s_\beta}\sigma_x^{s_\gamma}\sigma_z\cdots\sigma_z\sigma_x^{s_\delta} \\ - & + & + & \sigma_x\cdots\sigma_x \quad \sigma_y\cdots\sigma_y \\ + & - & + & \sigma_x\cdots\sigma_y \quad \sigma_x\cdots\sigma_y \\ + & + & - & \sigma_x\cdots\sigma_y \quad \sigma_y\cdots\sigma_x \\ + & + & - & \sigma_y\cdots\sigma_x \quad \sigma_x\cdots\sigma_y \\ + & - & + & \sigma_y\cdots\sigma_x \quad \sigma_y\cdots\sigma_x \\ - & + & + & \sigma_y\cdots\sigma_y \quad \sigma_x\cdots\sigma_x \\ + & + & + & \sigma_y\cdots\sigma_y \quad \sigma_y\cdots\sigma_y \end{cases} \tag{34}$$

where the letters I, II and III refer to the subgroups defined in Eq. (29).

As for the single-particle operators in subsection II D we now need to factorize these multi-qubit terms in the Hamiltonian to products of two-qubit and single-qubit operators. Instead of transforming a product of the form $az\cdots zb$, we now need to transform a product of the form $az\cdots zbcz\cdots zd$, where a, b, c and d are short for either σ_x or σ_y while z is short for σ_z. The generalization is quite straightforward, as we see that if the initial operator is $\sigma_z^{s_\alpha}\sigma_z^{s_\gamma}$ instead of just $\sigma_z^{s_\alpha}$, we can use the same set of transformations as for the single-particle case,

$$U_k^\dagger \cdots U_1^\dagger \sigma_z^{s_\alpha} U_1 \cdots U_k$$
$$= \sigma_a^{s_\alpha}\sigma_z\cdots\sigma_z\sigma_b^\beta$$
$$\Rightarrow \quad U_k^\dagger \cdots U_1^\dagger \sigma_z^{s_\alpha}\sigma_z^{s_\gamma} U_1 \cdots U_k$$
$$= \sigma_a^{s_\alpha}\sigma_z\cdots\sigma_z\sigma_b^{s_\beta}\sigma_z^{s_\gamma}. \tag{35}$$

Using the same unitary two-qubit transformations, which we now call V, that take $\sigma_z^{s_\gamma}$ to $\sigma_c^{s_\gamma}\sigma_z\cdots\sigma_z\sigma_d^{s_\delta}$, we find

$$V_s^\dagger\cdots V_1^\dagger U_k^\dagger\cdots U_1^\dagger\sigma_z^{s_\alpha}\sigma_z^{s_\gamma}U_1\cdots U_kV_1\cdots V_s$$
$$=\sigma_a^{s_\alpha}\sigma_z\cdots\sigma_z\sigma_b^\beta\sigma_c^{s_\gamma}\sigma_z\cdots\sigma_z\sigma_d^\delta. \quad (36)$$

This straightforward generalization of the procedure from the single-particle Hamiltonian case is possible because the operations commute when performed on different qubits.

With the above expressions, we can start with the unitary operator $\exp(-ia\sigma_z^{s_\alpha}\sigma_z^{s_\gamma})$ and have two different series of unitary operators that give us the evolution operator of the desired Hamiltonian. The U operators are defined as in Eq. (21),

$$e^{-i\sigma^{s_\alpha}\sigma_z\cdots\sigma_z\sigma^{s_\beta}a}=\left(\prod_k U_k^\dagger\right)e^{-i\sigma_z^{s_\alpha}a}\left(\prod_{k'}U_{k'}\right), \quad (37)$$

while the V operators are defined in a similar way

$$e^{-i\sigma^{s_\gamma}\sigma_z\cdots\sigma_z\sigma^{s_\delta}a}=\left(\prod_s V_s^\dagger\right)e^{-i\sigma_z^{s_\gamma}a}\left(\prod_{s'}V_{s'}\right), \quad (38)$$

where the σ-matrices without subscripts represent that we can have σ_x or σ_y in each position.

This gives us the total evolution operator for each term in Eq. (34)

$$e^{-i\sigma^{s_\alpha}\sigma_z\cdots\sigma_z\sigma^{s_\beta}\sigma^{s_\gamma}\sigma_z\cdots\sigma_z\sigma^{s_\delta}a}$$
$$=\left(\prod_s V_s^\dagger\right)\left(\prod_k U_k^\dagger\right)e^{-i\sigma_z^{s_\alpha}\sigma_z^{s_\gamma}a}$$
$$\times\left(\prod_{k'}U_{k'}\right)\left(\prod_{s'}V_{s'}\right). \quad (39)$$

Here we have all the single- and two-qubit operations we need to perform on our set of qubits, that were initially in the state $|\psi\rangle$, to simulate the time evolution $\exp(-iH_k\Delta t)|\psi\rangle$ of the Hamiltonian term $H_k=\sigma^{s_\alpha}\sigma_z\cdots\sigma_z\sigma^{s_\beta}\sigma^{s_\gamma}\sigma_z\cdots\sigma_z\sigma^{s_\delta}$. Every factor in the above equation is a single- or two-qubit operation that must be performed on the qubits in proper matrix multiplication order.

When using the Jordan-Wigner transformation of Eq. (11) applied to our two model Hamiltonians of Eqs. (2) and (3), we choose a representation with two qubits at each site. These correspond to fermions with spin up and down, respectively. The number of qubits, n, is always the total number of available quantum states and therefore it is straightforward to use this model on systems with higher degeneracy, such as those encountered in quantum chemistry [3] or nuclear physics [16]. Site one spin up is qubit one, site one spin down is qubit two and site two spin up is qubit three and so on. To get all the quantum gates one needs to simulate a given Hamiltonian one needs to input the correct E_{ij} and V_{ijkl} values.

F. Complexity of the quantum computing algorithm

In order to test the efficiency of a quantum algorithm, one needs to know how many qubits, and how many operations on these, are needed to implement the algorithm. Usually this is a function of the dimension of the Hilbert space on which the Hamiltonian acts. The natural input scale in the fermionic simulator is the number of quantum states, n, that are available to the fermions. In our simulations of the Hubbard and the pairing models of Eqs. (2) and (3), respectively, the number of qubits is $n=2N$ since we have chosen systems with double-degeneracy for every single-particle state, where N is the number of energy-levels in the model. We use one qubit to represent each possible fermion state, on a real quantum computer, however, one should implement some error-correction procedure using several qubits for each state, see Ref. [37]. The complexity in number of qubits remains linear, however, since $\mathcal{O}(n)$ qubits are needed for error correction.

The single-particle Hamiltonian has potentially $\mathcal{O}(n^2)$ different E_{ij} terms. The two-particle Hamiltonian has up to $\mathcal{O}(n^4)$ V_{ijkl} terms. A general m-body interaction has in the worst case $\mathcal{O}(n^{2m})$ terms. It is straightforward to convince oneself that the pairing model has $\mathcal{O}(n^2)$ terms while in the Hubbard model we end up with $\mathcal{O}(n)$ terms. Not all models have maximum complexity in the different m-body interactions.

How many two-qubit operations do each of these terms need to be simulated? First of all a two-qubit operation will in general have to be decomposed into a series of universal single- and two-qubit operations, depending entirely on the given quantum simulator. A particular physical realization might have a natural implementation of the $\sigma_z^i\otimes\sigma_z^j$ gate and save a lot of intermediary operations. Others will have to use a fixed number of operations in order to apply the operation on any two qubits. A system with only nearest neighbor interactions would have to use $\mathcal{O}(n)$ operations for each $\sigma_z^i\otimes\sigma_z^j$ gate, and thereby increase the polynomial complexity by one degree.

In our discussion on the one-body part of the Hamiltonian, we saw that for each E_{ij} we obtained the $a_i^\dagger a_j+a_j^\dagger a_i$ operator which is transformed into the two terms in Eq. (16), $\sigma_x\sigma_z\cdots\sigma_z\sigma_x$ and $\sigma_y\sigma_z\cdots\sigma_z\sigma_y$. We showed how these terms are decomposed into $j-i+2$ operations, leading to twice as many unitary transformations on an operator, $VAV^\dagger$ for the time evolution. The average of $j-i$ is $n/2$ in this case and in total we need to perform $2\times2\times n/2=2n$ two-qubit operations per single-particle term in the Hamiltonian, a linear complexity.

In the two-particle case each term $V_{ijkl}(a_i^\dagger a_j^\dagger a_l a_k+a_k^\dagger a_l^\dagger a_j a_i)$ is transformed into a sum of eight operators of the form $\sigma^{s_\alpha}\sigma_z\cdots\sigma_z\sigma^{s_\beta}\sigma^{s_\gamma}\sigma_z\cdots\sigma_z\sigma^{s_\delta}$, Eq. (34). The two parts of these operators are implemented in the same way as the $\sigma^i\sigma_z\cdots\sigma_z\sigma^j$ term of the single-particle Hamil-

tonian, which means they require $s_\beta - s_\alpha$ and $s_\delta - s_\gamma$ operations, since $s_\alpha < s_\beta < s_\gamma < s_\delta$ the average is $n/4$. For both of these parts we need to perform both the unitary operation V and it's Hermitian conjugate $V^\dagger$. In the end we need $2 \times 2 \times 8 \times n/4 = 8n$ two-qubit operations per two-particle term in the Hamiltonian, the complexity is linear.

A term of an m-body Hamiltonian will be transformed into 2^{2m} operators since each annihilation and creation operator is transformed into a sum of σ_x and σ_y matrices. All the imaginary terms cancel out and we are left with 2^{2m-1} terms. Each of these terms will include $2m$ σ matrices, in products of the form $\prod_{k=1}^{m} \sigma^i \sigma_z \cdots \sigma_z \sigma^j$, and we use the same procedure as discussed above to decompose these m factors into unitary transformations. In this case each factor will require an average of $n/2m$ operations for the same reasons as in the two-body case. All in all, each m-body term in the Hamiltonian requires $2^{2m-1} \times 2 \times m \times n/2m = 2^{2m-1}n$ operations.

Thus, the complexity for simulating one m-body term of a fermionic many-body Hamiltonian is linear in the number of two-qubit operations, but the number of terms is not. For a full-fledged simulation of general three-body forces, in common use in nuclear physics [40, 41, 42], the total complexity of the simulation is $\mathcal{O}(n^7)$. A complete two-particle Hamiltonian would be $\mathcal{O}(n^5)$. The bottleneck in these simulations is the number of terms in the Hamiltonian, and for systems with less than the full number of terms the simulation will be faster. This is much better than the exponential complexity of most simulations on classical computers.

III. ALGORITHMIC DETAILS

Having detailed how a general Hamiltonian, of two-body nature in our case, can be decomposed in terms of various quantum gates, we present here details of the implementation of our algorithm for finding eigenvalues and eigenvectors of a many-fermion system. For our tests of the fermionic simulation algorithm we have implemented the phase-estimation algorithm from [37] which finds the eigenvalues of an Hamiltonian operating on a set of simulation qubits. There are also other quantum computer algorithms for finding expectation values and correlation functions, as discussed by Somma *et al.* in Refs. [25, 26]. In the following we first describe the phase-estimation algorithm, and then describe its implementation and methods we have developed in using this algorithm. A much more thorough description of quantum computers and the phase-estimation algorithm can be found in [43].

A. Phase-estimation algorithm

To find the eigenvalues of the Hamiltonian we use the unitary time evolution operator we get from the Hamiltonian. We have a set of simulation qubits representing the system governed by the Hamiltonian, and a set of auxiliary qubits, called work qubits [20, 21], in which we will store the eigenvalues of the time evolution operator. The procedure is to perform several controlled time evolutions with work qubits as control qubits and the simulation qubits as targets, see for example Ref. [37] for information on controlled qubit operations. For each work qubit we perform the controlled operation on the simulation qubits with a different time parameter, giving all the work qubits different phases. The information stored in their phases is extracted using first an inverse Fourier transform on the work qubits alone, and then performing a measurement on them. The values of the measurements give us directly the eigenvalues of the Hamiltonian after the algorithm has been performed a number of times.

The input state of the simulation qubits is a random state in our implementation, which is also a random superposition of the eigenvectors of the Hamiltonian $|\psi\rangle = \sum_k c_k |k\rangle$. It does not have to be a random state, and in [44] the authors describe a quasi-adiabatic approach, where the initial state is created by starting in the ground state for the non-interacting Hamiltonian, a qubit basis state, e.g. $|0101 \cdots 101\rangle$, and then slowly the interacting part of the Hamiltonian is turned on. This gives us an initial state mostly comprising the true ground state, but it can also have parts of the lower excited states if the interacting Hamiltonian is turned on a bit faster. In for example nuclear physics it is common to use a starting state for large-scale diagonalizations that reflects some of the features of the states one wishes to study. A typical example is to include pairing correlations in the trial wave function, see for example Refs. [16, 34]. Iterative methods such as the Lanczo's diagonalization technique [19, 45] converge much faster if such starting vectors are used. However, although more iterations are needed, even a random starting vector converges to the wanted states.

The final state of all the qubits after an inverse Fourier transform on the work qubits is

$$\sum_k c_k |\phi^{[k]} 2^t\rangle \otimes |k\rangle. \tag{40}$$

If the algorithm works perfectly, $|k\rangle$ should be an exact eigenstate of U, with an exact eigenvalue $\phi^{[k]}$. When we have the eigenvalues of the time evolution operator we easily find the eigenvalues of the Hamiltonian. We can summarize schematically the phase-estimation algorithm as follows:

1. Intialize each of the work qubits to $1/\sqrt{2}(|0\rangle + |1\rangle)$ by initializing to $|0\rangle$ and applying the Hadamard gate, H, see Fig. 2.

2. Initialize the simulation qubits to a random or specified state, depending on the whether one wants the whole eigenvalue spectrum.

3. Perform conditional time evolutions on the simulation qubits, with different timesteps Δt and different work qubits as the control qubits.
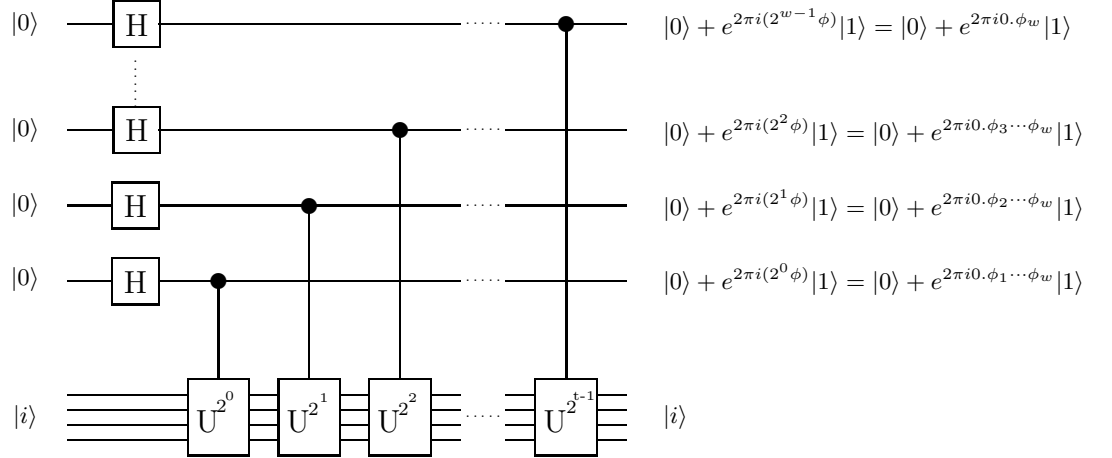
FIG. 3: Phase estimation circuit showing all the different qubit lines schematically with operations represented by boxes. The boxes connected by vertical lines to other qubit lines are controlled operations, with the qubit with the black dot as the control qubit.

4. Perform an inverse Fourier transform on the work qubits.

5. Measure the work qubits to extract the phase.

6. Repeat steps 1-6 until the probability distribution

gathered from the measurement results is good enough to read out the wanted eigenvalues.

As discussed above a set of two-qubit operations can be simulated by the CNOT two-qubit operation and a universal set of single-qubit operations. We will not use or discuss any such implementation in this article, as one will have to use a different set for each physical realization of a quantum computer. When simulating a fermion system with a given quantum computer, our algorithm will first take the fermionic many-body evolution operator to a series of two-qubit and single-qubit operations, and then one will have to have a system dependent setup that takes these operations to the basic building blocks that form the appropriate universal set.

In subsection II E we showed how to take any two-particle fermionic Hamiltonian to a set of two-qubit operations that approximate the evolution operator. In addition we must use one of the Trotter approximations [46, 47, 48] Eqs. (6) and (41) that take the evolution operator of a sum of terms to the product of the evolution operator of the individual terms, see for example Ref. [37] for details. To order $\mathcal{O}(\Delta t^2)$ in the error we use Eq. (6) while to order $\mathcal{O}(\Delta t^3)$ we have

$$e^{-i(A+B)\Delta t} = e^{-iA\Delta t/2}e^{-iB\Delta t}e^{-iA\Delta t/2} + \mathcal{O}(\Delta t^3). \quad (41)$$

B. Output of the phase-estimation algorithm

The output of the phase-estimation algorithm is a series of measurements of the w number of work qubits. Putting them all together we get a probability distribution that estimates the amplitudes $|c_k|^2$ for each eigenvalue $\phi^{[k]}$. The $\phi^{[k]}2^w$ values we measure from the work qubits, see Eq. (40), are binary numbers from zero to $2^w - 1$, where each one translates to a given eigenvalue of the Hamiltonian depending on the parameters we have used in our simulation. When accurate, a set of simulated measurements will give a distribution with peaks around the true eigenvalues. The probability distribution is calculated by applying non-normalized projection operators to the qubit state,

$$\left(|\phi^{[k]}2^t\rangle\langle\phi^{[k]}2^t| \otimes \mathbf{1} \right) \left(\sum_i c_i|\phi_i 2^t\rangle \otimes |i\rangle \right) = c_k|\phi^{[k]}2^t\rangle \otimes |k\rangle.$$

The length of this vector squared gives us the probability,

$$\left| c_k|\phi^{[k]}\rangle 2^t \otimes |k\rangle \right|^2 = |c_k|^2 \langle\phi^{[k]}2^t|\phi^{[k]}2^t\rangle\langle k|k\rangle = |c_k|^2. \quad (42)$$

Since we do not employ the exact evolution due to different approximations, we can have non-zero probabilities

for all values of ϕ, yielding a distribution without sharp peaks for the correct eigenvalues and possibly peaks in the wrong places. If we use different random input states for every run through the quantum computer and gather all the measurements in one probability distribution, all the eigenvectors in the input state $|\psi\rangle = \sum_k c_k |k\rangle$ should average out to the same amplitude. This means that eigenvalues with higher multiplicity, i.e., higher degeneracy, will show up as taller peaks in the probability distribution, while non-degenerate eigenvalues might be difficult to find.

To properly estimate the eigenvalues E_k of the Hamiltonian from this distribution, one must take into account the periodicity of $e^{2\pi i \phi}$. If $0 < \phi' < 1$ and $\phi = \phi' + s$, where s is an integer, then $e^{2\pi i \phi} = e^{2\pi i \phi'}$. This means that to get all the eigenvalues correctly ϕ must be positive and less than one. Since $\phi = -E_k \Delta t / 2\pi$ this means all the eigenvalues E_k must be negative, this merely means subtracting a constant we denote E_{max} from the Hamiltonian, $H' = H - E_{max}$, where E_{max} is greater than the largest eigenvalue of H. The values we read out from the work qubits are integers from zero to $2^w - 1$. In other words, we have $\phi^{[k]} 2^w \in [0, 2^w - 1]$, with $\phi = 0$ for $\Delta t = 0$.

The value $\phi = 0$ corresponds to the lowest eigenvalue possible to measure, E_{min}, while $\phi = 1$ corresponds to E_{max}. The interval of possible values is then $E_{max} - E_{min} = 2\pi / \Delta t$. If we want to have all possible eigenvalues in the interval the largest value Δt can have is

$$\max(\Delta t) = \frac{2\pi}{E_{max} - E_{min}} \qquad (43)$$

1. Spectrum analysis

In the general case one does not know the upper and lower bounds on the eigenvalues beforehand, and therefore for a given E_{max} and Δt one does not know if the $\phi^{[k]}$ values are the correct ones, or if an integer has been lost in the exponential function.

When $\phi = \phi' + s$ for one Δt, and we slightly change Δt, ϕ' will change if $s \neq 0$ as the period of the exponential function is a function of Δt. To find out which of $\phi^{[k]}$s are greater than one, we perform the phase-estimation algorithm with different values for Δt and see which eigenvalues shift. If we measure the same ϕ after adding δt to the time step, and $(\Delta t + \delta t)/\Delta t$ is not a rational number, we know that $\phi < 1$. In practice it does not have to be an irrational number, but only some unlikely fraction.

There are at least two methods for finding the eigenvalues. One can start with a large positive E_{max} and a small Δt, hoping to find that the whole spectrum falls within the range $[E_{min}, E_{max}]$, and from there zoom in until the maximal eigenvalue is slightly less than E_{max} and the groundstate energy is slightly larger than E_{min}. This way the whole spectrum is covered at once. From there we can also zoom in on specific areas of the spectrum, searching the location of the true eigenvalues by shifting Δt.

The number of measurements needed will depend entirely on the statistics of the probability distribution. The number of eigenvalues within the given energy range determines the resolution needed. That said, the number of measurements is not a bottleneck in quantum computer calculations. The quantum computer will prepare the states, apply all the operations in the circuit and measure. Then it will do it all again. Each measurement will be independent of the others as the system is restarted each time. This way the serious problem of decoherence only apply within each run, and the number of measurements is only limited by the patience of the scientists operating the quantum computer.

IV. RESULTS AND DISCUSSION

In this section we present the results for the Hubbard model and the pairing model of Eqs. (2) and (3), respectively, and compare the simulations to exact diagonalization results. In Fig. 4 we see the resulting probability distribution from the simulated measurements, giving us the eigenvalues of the pairing model with six degenerate energy levels and from zero to 12 particles. The pairing strength was set to $g = 1$. The eigenvalues from the exact solutions of these many-particle problems are 0, -1, -2, -3, -4, -5, -6, -8, -9, -12. All the eigenvalues are not seen as this is the probability distribution resulting from one random input state. A different random input state in each run could be implemented on an actual quantum computer. These are results for the degenerate model, where the single-particle energies of the doubly degenerate levels are set to zero for illustrate purposes only, since analytic formula are available for the exact eigenvalues. The block diagonal structure of the pairing Hamiltonian has not been used to our advantage in this straightforward simulation as the qubit basis includes all particle numbers.

We have also performed tests of the algorithm for the non-degenerate case, with excellent agreement with our diagonalization codes, see discussion in Ref. [34]. This is seen in Fig. 5 where we have simulated the pairing model with four energy levels with a total possibility of eight fermions. We have chosen $g = 1$ and $d = 0.5$, so this is a model with low degeneray and since the dimension of the system is $2^8 = 256$ there is a lot of different eigenvalues. To find the whole spectrum one would have to employ some of the techniques discussed in subsection III B.

A. Number of work qubits versus number of simulation qubits

The largest possible amount of different eigenvalues is 2^s, where s is the number of simulation qubits. The
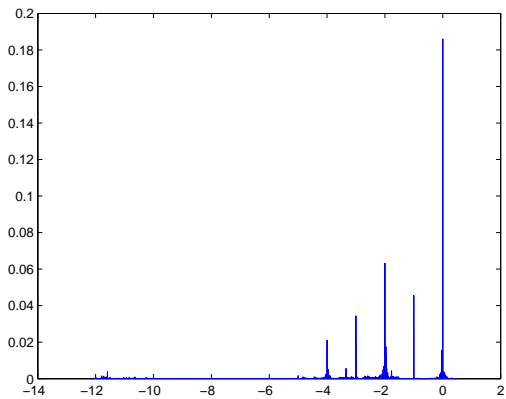
FIG. 4: Resulting probability distribution from the simulated measurements, giving us the eigenvalues of the pairing model with six degenerate energy levels with a total possibility of 12 particles and pairing strength $g = 1$. The correct eigenvalues are 0, -1, -2, -3, -4, -5, -6, -8, -9, -12. All the eigenvalues are not seen as this is the probability distribution resulting from one random input state. A different random input state in each run could be implemented on an actual quantum computer and would eventually yield peaks of height corresponding to the degeneracy of each eigenvalue.
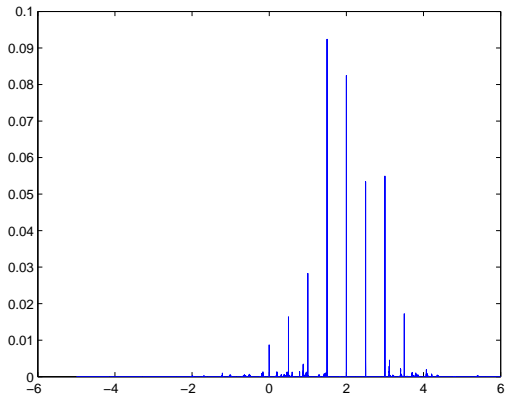

FIG. 5: The eigenvalues of the non-degenerate pairing model with four energy levels with a total possibility of 8 particles, the level spacing d is 0.5 and the pairing strength g is 1. The correct eigenvalues are obtained from exact diagonalization, but in this case there is a multitude of eigenvalues and only some eigenvalues are found from this first simulation.

resolution in the energy spectrum we get from measuring upon the work qubits is 2^w, with w the number of work qubits. Therefore the resolution per eigenvalue in a non-degenerate system is 2^{w-s}. The higher the degeneracy the less work qubits are needed.

In Fig. 6 we see the results for the Hubbard model Eq. (2) with $\epsilon = 1$, $t = 0$ and $U = 1$. The reason we

chose $t = 0$ was just because of the higher degeneracy and therefore fewer eigenvalues. The number of work qubits is 16 and the number of simulation qubits is eight for a total of 24 qubits. The difference between work qubits and simulation qubits is eight which means there are 2^8 possible energy values for each eigenvalue. Combining that with the high degeneracy we get a very sharp resolution. The correct eigenvalues with degeneracies are obtained from exact diagonalization of the Hamiltonian, the degeneracy follows the eigenvalue in paranthesis: 0(1), 1(8), 2(24), 3(36), 4(40), 5(48), 6(38), 7(24), 8(24), 9(4), 10(8), 12(1). We can clearly see that even though we have a random input state, with a random superposition of the eigenvectors, there is a correspondence between the height of the peaks in the plot and the degeneracy of the eigenvalues they represent.
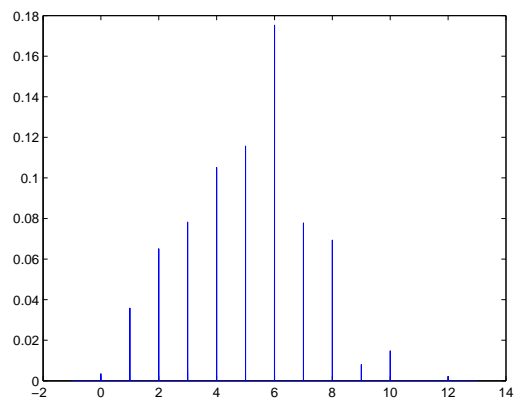

FIG. 6: The energy levels of the Hubbard model of Eq. (2), simulated with a total of 24 qubits, of which eight were simulation qubits and 16 were work qubits. In this run we chose $\epsilon = 1$, $t = 0$ and $U = 1$. The reason we chose $t = 0$ was just because of the higher degeneracy and therefore fewer eigenvalues. The correct eigenvalues are obtained from exact diagonalization, with the level of degeneracy following in paranthesis: 0(1), 1(8), 2(24), 3(36), 4(40), 5(48), 6(38), 7(24), 8(24), 9(4), 10(8), 12(1).

B. Number of time intervals

The number of time intervals, I, is the number of times we must implement the time evolution operator in order to reduce the error in the Trotter approximation [46, 47, 48], see Eq. (6). In our program we have only implemented the simplest Trotter approximation and in our case we find that we do not need a large I before the error is small enough. In Fig. 6 I is only one, but here we have a large number of work qubits. For other or larger systems it might pay off to use a higher order Trotter approximation. The total number of operations that have to be done is a multiple of I, but this number

also increases for higher order Trotter approximations, so for each case there is an optimal choice of approximation.

In Figs. 7 and 8 we see the errors deriving from the Trotter approximation, and how they are reduced by increasing the number of time intervals. The results in this figure are for the degenerate pairing model with 24 qubits in total, and ten simulation qubits with $d = 0$ and $g = 1$. In Fig. 7 we had $I = 1$ while in Fig. 8 I was set to ten. Both simulations used the same starting state. The errors are seen as the small spikes around the large ones which represent some of the eigenvalues of the system. The exact eigenvalues are 0, -1, -2, -3, -4, -5, -6, -8, -9.
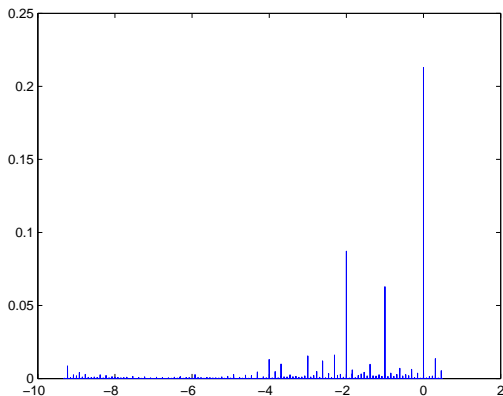

FIG. 8: Pairing model simulated with 24 qubits, where 14 were simulation qubits, i.e. there are 14 available quantum levels, and 10 were work qubits. The correct eigenvalues are 0, -1, -2, -3, -4, -5, -6, -8, -9. In this run we divided the time interval into 10 equally space parts in order to reduce the error in the Trotter approximation, i.e., $I = 10$.

	$s = 2$	$s = 4$	$s = 6$	$s = 8$	$s = 10$	$s = 12$
H_P	9	119	333	651	1073	1598
H_H	9	51	93	135	177	219

TABLE I: Number of two-qubit gates used in simulating the time evolution operator of the pairing model, H_P, and the Hubbard model, H_H, for different number of simulation qubits s.
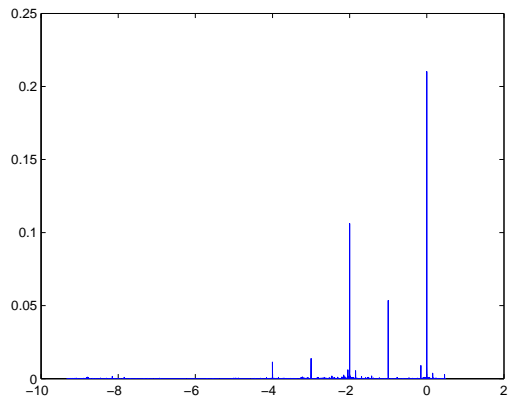

FIG. 7: Pairing model simulated with 24 qubits, where 14 were simulation qubits, i.e. there are 14 available quantum levels, and 10 were work qubits. The correct eigenvalues are 0, -1, -2, -3, -4, -5, -6, -8, -9. In this run we did not divide up the time interval to reduce the error in the Trotter approximation, i.e., $I = 1$.

C. Number of operations

Counting the number of single-qubit and $\sigma_z\sigma_z$ operations for different sizes of systems simulated gives us an indication of the decoherence time needed for different physical realizations of a quantum simulator or computer. The decoherence time is an average time in which the state of the qubits will be destroyed by noise, also called decoherence, while the operation time is the average time an operation takes to perform on the given system. Their fraction is the number of operations possible to perform before decoherence destroys the computation. In table I we have listed the number of gates used for the pairing model, H_P, and the Hubbard model, H_H, for different number of simulation qubits.

V. CONCLUSION

In this article we have shown explicitly how the Jordan-Wigner transformation is used to simulate any many-body fermionic Hamiltonian by two-qubit operations. We have shown how the simulation of such Hamiltonian terms of products of creation and annihilation operators are represented by a number of operations linear in the number of qubits. To perform efficient quantum simulations on quantum computers one needs transformations that take the Hamiltonian in question to a set of operations on the qubits simulating the physical system. An example of such a transformation employed in ths work, is the Jordan-Wigner transformation. With the appropriate transformation and relevant gates or quantum circuits, one can taylor an actual quantum computer to simulate and solve the eigenvalue and eigenvector problems for different quantum systems. Specialized quantum simulators might be more efficient in solving some problems than others because of similarities in algebras between physical system of qubits and the physical system simulated.

We have limited the applications to two simple and well-studied models that provide, via exact eigenvalues,

a good testing ground for our quantum computing based algorithm. For both the pairing model and the Hubbard model we obtain an excellent agreement. We plan to extend the area of application to quantum mechanical studies of systems in nuclear physics, such as a comparison of shell-model studies of oxygen or calcium isotopes where the nucleons are active in a given number of single-particle orbits [7, 16]. These single-particle orbits have normally a higher degeneracy than 2, a degeneracy studied here. However, the algorithm we have developed allows for the inclusion of any degeneracy, meaning in turn that with a given interaction V_{ijkl} and single-particle energies, we can compare the nuclear shell-model (configuration interaction) calculations with our algorithm.

Acknowledgment

APPENDIX: USEFUL RELATIONS

We list here some useful relations involving different σ matrices,

$$\sigma_x\sigma_z = -i\sigma_y, \quad \sigma_z\sigma_x = i\sigma_y, \quad [\sigma_x,\sigma_z] = -2i\sigma_y, \quad (A.1)$$

$$\sigma_x\sigma_y = i\sigma_z, \quad \sigma_y\sigma_x = -i\sigma_z, \quad [\sigma_x,\sigma_y] = 2i\sigma_z, \quad (A.2)$$

and

$$\sigma_y\sigma_z = i\sigma_x, \quad \sigma_z\sigma_y = -i\sigma_x, \quad [\sigma_y,\sigma_z] = 2i\sigma_x. \quad (A.3)$$

For any two non-equal σ-matrices a and b we have

$$aba = -b. \quad (A.4)$$

The Hermitian σ-matrices σ_x, σ_y and σ_z result in the identity matrix when squared

$$\sigma_x^2 = \mathbf{1}, \quad \sigma_y^2 = \mathbf{1}, \quad \sigma_z^2 = \mathbf{1}, \quad (A.5)$$

which can be used to obtain simplified expressions for exponential functions involving σ-matrices

$$e^{\pm i\alpha\sigma} = \cos(\alpha)\mathbf{1} \pm i\sin(\alpha)\sigma. \quad (A.6)$$

The equations we list below are necessary for the relation between a general unitary transformation on a set of qubits with a product of two-qubit unitary transformations. We have the general equation for $a, b \in \{\sigma_x, \sigma_y, \sigma_z\}$, where $a \neq b$.

$$
\begin{aligned}
e^{-i\pi/4a}be^{i\pi/4a} &= \frac{1}{2}(\mathbf{1} - ia)b(\mathbf{1} + ia) \\
&= \frac{1}{2}(b + aba + i[b,a]) \\
&= \frac{i}{2}[b,a]. \quad (A.7)
\end{aligned}
$$

The more specialized equations read

$$e^{-i\pi/4\sigma_x}\sigma_z e^{i\pi/4\sigma_x} = -\sigma_y, \quad (A.8)$$
$$e^{-i\pi/4\sigma_y}\sigma_z e^{i\pi/4\sigma_y} = \sigma_x, \quad (A.9)$$
$$e^{-i\pi/4\sigma_z}\sigma_x e^{i\pi/4\sigma_z} = \sigma_y, \quad (A.10)$$
$$e^{-i\pi/4\sigma_z}\sigma_y e^{i\pi/4\sigma_z} = -\sigma_x. \quad (A.11)$$

We need also different products of the operator σ_z with the raising and lowering operators

$$\sigma_+\sigma_z = -\sigma_+ \quad (A.12)$$
$$\sigma_z\sigma_+ = \sigma_+, \quad (A.13)$$
$$\sigma_-\sigma_z = \sigma_-, \quad (A.14)$$
$$\sigma_z\sigma_- = -\sigma_-. \quad (A.15)$$
$$(A.16)$$

[1] R. J. Bartlett. Many-body perturbation theory and coupled-cluster theory for electron correlations in molecules. *Ann. Rev. Phys. Chem.*, 32:359, 1981.

[2] D. J. Dean and M. Hjorth-Jensen. Coupled-cluster approach to nuclear physics. *Phys. Rev. C*, 69:054320, 2004.

[3] T. Helgaker, P. Jørgensen, and J. Olsen. *Molecular Electronic Structure Theory. Energy and Wave Functions.* Wiley, Chichester, 2000.

[4] D. M. Ceperley. Path integrals in the theory of condensed helium. *Rev. Mod. Phys.*, 67:279, 1995.

[5] S.E. Koonin, D.J. Dean, and K. Langanke. *Phys. Rep.*, 278:1, 1997.

[6] B. S. Pudliner, V. R. Pandharipande, J. Carlson, Steven C. Pieper, and R. B. Wiringa. Quantum monte carlo calculations of nuclei with $A \leq 7$. *Phys. Rev. C*, 56:1720, 1997.

[7] M. Hjorth-Jensen, T. T. S. Kuo, and E. Osnes. Realistic effective interactions for nuclear systems. *Phys. Rep.*, 261:125, 1995.

[8] I. Lindgren and J. Morrison. *Atomic Many-Body Theory.* Springer, Berlin, 1985.

[9] J. P. Blaizot and G. Ripka. *Quantum theory of Finite Systems.* MIT press, Cambridge, USA, 1986.

[10] W. H. Dickhoff and D. Van Neck. *Many-Body Theory exposed!* World Scientific, 2005.

[11] U. Schollwock. The density-matrix renormalization group. *Rev. Mod. Phys.*, 77:259, 2005.

[12] S. R. White. Density matrix formulation for quantum renormalization groups. *Phys. Rev. Lett.*, 69:2863, 1992.

[13] R. J. Bartlett, V. F. Lotrich, and I. V. Schweigert. Ab initio density functional theory: The best of both worlds? *J. Chem. Phys.*, 123:062205, 2005.

[14] D. Van Neck, S. Verdonck, G. Bonny, P. W. Ayers, and M. Waroquier. Quasiparticle properties in a density-functional framework. *Phys. Rev. A*, 74:042501, 2006.

[15] K. Peirs, D. Van Neck, and M. Waroquier. Algorithm to derive exact exchange-correlation potentials from correlated densities in atoms. *Phys. Rev. A*, 67:012505, 2003.

[16] E. Caurier, G. Martinez-Pinedo, F. Nowacki, A. Poves, and A. P. Zuker. The shell model as a unified view of nuclear structure. *Rev. Mod. Phys.*, 77:427, 2005.

[17] M. Horoi, B. A. Brown, T. Otsuka, M. Honma, and T. Mizusaki. Shell model analysis of the ^{56}Ni spectrum in the full pf model space. *Phys. Rev. C*, 73:061305, 2006.

[18] P. Navratil and E. Caurier. Nuclear structure with accurate chiral perturbation theory nucleon-nucleon potential: Application to ^{6}Li and ^{10}B. *Phys. Rev. C*, 69:014311, 2004.

[19] R. R. Whitehead, A. Watt, B. J. Cole, and I. Morrison. Computational methods for shell-model calculations. *Adv.Nucl.Phys.*, 9:123, 1977.

[20] D. S. Abrams and S. Lloyd. Simulation of many-body fermi systems on a universal quantum computer. *Phys. Rev. Lett.*, 79:2586, 1997.

[21] D. S. Abrams and S. Lloyd. Quantum algorithm providing exponential speed increase for finding eigenvalues and eigenvectors. *Phys. Rev. Lett.*, 83:5162, 1999.

[22] R. P. Feynman. Simulating physics with computers. *Int. J. Theor. Phys.*, 21:467, 1982.

[23] R. P. Feynman. Quantum mechanical computers. *Foundations. Phys.*, 16:507, 1986.

[24] G. Ortiz, J. E. Gubernatis, E. Knill, and R. Laflamme. Simulating fermions on a quantum computer. *Comp. Phys. Comm.*, 146:302, 2002.

[25] R. Somma, G. Ortiz, J. E. Gubernatis, E. Knill, and R. Laflamme. Simulating physical phenomena by quantum networks. *Phys. Rev. A*, 65:042323, 2002.

[26] R. D. Somma. *Quantum Computation, Complexity, and Many-Body Physics*. PhD thesis, Instituto Balseiro, S.C. de Bariloche, Argentina and Los Alamos National Laboratory, Los Alamos, U.S.A., 2005.

[27] K. R. Brown, R. J. Clark, and I. L. Chuang. Limitations of quantum simulation examined by simulating a pairing hamiltonian using nuclear magnetic resonance. *Phys. Rev. Lett.*, 97:050504, 2006.

[28] X. Yang, A. Wang, F. Xu, and J. Du. Experimental simulation of a pairing hamiltonian on an NMR quantum computer. *Chem. Phys. Lett.*, 422:20, 2006.

[29] J. Hubbard. Electron correlations in narrow energy bands. *Proc. R. Soc. A*, 276:238, 1963.

[30] I. Talmi. *Simple Models of Complex Nuclei*. Harwood Academic Publishers, 1993.

[31] R. W. Richardson. A restricted class of exact eigenstates of the pairing-force Hamiltonian *Phys. Lett.*, 3:277, 1963.

[32] R. W. Richardson and N. Sherman. Exact Eigenstates of the Pairing-Force Hamiltonian. I *Nucl. Phys.*, 52:221, 1964.

[33] R. W. Richardson. Exact Eigenstates of the Pairing-Force Hamiltonian. II *J. Math. Phys.*, 6:1034, 1965.

[34] D. J. Dean and M. Hjorth-Jensen. Pairing in nuclear systems: from neutron stars to finite nuclei. *Rev. Mod. Phys.*, 75:607, 2003.

[35] J. Dukelsky, S. Pittel, and G. Sierra. Exactly solvable Richardson-Gaudin models for many-body quantum systems. *Rev. Mod. Phys.*, 76:643, 2004.

[36] P.Benioff. The computer as a physical system: A microscopic quantum mechanical hamiltonian model of computers as represented by turing machines. *J. Stat. Phys.*, 22:563, 1980.

[37] M. A. Nielsen and I. L. Chaung. *Quantum Computation and Quantum Information*. Cambridge University Press, 2000.

[38] G. Ortiz, J. E. Gubernatis, E. Knill, and R. Laflamme. Quantum algorithms for fermionic simulations. *Phys. Rev. A*, 64:022319, 2001.

[39] P. Dargis and Z. Maassarani. Fermionization and Hubbard models. *Nucl. Phys. B*, 535:681, 1998.

[40] Steven C. Pieper, V. R. Pandharipande, R. B. Wiringa, and J. Carlson. Realistic models of pion-exchange three-nucleon interactions. *Phys. Rev. C*, 64:014001, 2001.

[41] P. Navrátil and W. E. Ormand. Ab initio shell model calculations with three-body effective interactions for *p*-shell nuclei. *Phys. Rev. Lett.*, 88:152502, 2002.

[42] G. Hagen, T. Papenbrock, D. J. Dean, A. Schwenk, M. Włoch, P. Piecuch, and A. Nogga. Coupled-cluster theory for three-body hamiltonians. arXiv:nucl-th/0704.2854, 2007.

[43] E. Ovrum. Quantum computing and many-body physics. Master's thesis, University of Oslo, 2003.

[44] L.-A. Wu, M. S. Byrd, and D. A. Lidar. Polynomial-time simulation of pairing models on a quantum computer. *Phys. Rev. Lett.*, 89:057904, 2002.

[45] G.H. Golub and C.F. Van Loan. *Matrix Computations*. John Hopkins University Press, 1996.

[46] H. F. Trotter. On the product of semi-groups of operators. *Proc. Am. Math. Soc.*, 10:545, 1959.

[47] M. Suzuki. Transfer-matrix method and monte carlo simulation in quantum spin systems. *Phys. Rev. B*, 31:2957, Mar 1985.

[48] M. Suzuki. Decomposition formulas of exponential operators and Lie exponentials with some applications to quantum mechanics and statistical physics. *J. Math. Phys.*, 26:601, 1985.